Proton-nucleus scattering and density dependent meson masses in the nucleus

G. E. Brown
Physics Department, State University of New York, Stony Brook, New York 11794

A. Sethi and N. M. Hintz
School of Physics and Astronomy, University of Minnesota, Minneapolis, Minnesota 55455
(Received 19 June 1989; revised manuscript received 29 January 1991)

The influence of density dependent meson masses, proposed in many previous papers, on proton-nucleus scattering in the several hundred MeV region is investigated. Introduction of this density dependence is found to remove the nuclear radius discrepancy which persistently occurred in analysis with the nonrelativistic impulse approximation when empirical nuclear densities obtained from electron scattering were employed. Nonlocality, suggested by earlier derivations of the density dependent masses, had to be introduced. Taking the estimated range of nonlocality from the earlier calculations, agreement with experiment was significantly improved by this introduction. Effects on the spin-orbit interaction and imaginary part of the optical model are qualitatively discussed. The density dependent meson masses aid in increasing the strength of the spin-orbit interaction. Preliminary results calculated in a relativistic impulse approximation (IA2) formalism for the spin observables are shown and discussed.

I. INTRODUCTION

In a number of papers [1–5] it has been suggested that mesons masses, in the nuclear medium, decrease at about the same relative rate with increasing density as the nucleon effective mass m_N^*. Such a decrease in the scalar meson mass was motivated by calculations in the Nambu-Jona-Lasinio (NJL) model [6]. For the vector meson mass, results of these calculations were not so clear [7], but by scaling the cutoff Λ, the mass could be made to decrease. Adami and Brown [8] have shown that scaling Λ^*/Λ as m_S^*/m_S is necessary in NJL if the contact scalar interaction there is generalized to a finite range one. Using the quantum-chromodynamic (QCD) sum rules, Brown [9] showed that, to a good approximation, there is only one scale in the broken symmetry mode of QCD, and that this can be taken to be the pion decay constant f_π^*, which is the order parameter of the broken symmetry regime. Thus, all masses except for that of the pion (and kaon) made up out of up and down quarks should scale as

$$\frac{f_\pi^*}{f_\pi} \cong \frac{m_N^*}{m_N} \cong \frac{m_V^*}{m_V} \cong \frac{m_S^*}{m_S} \cong \frac{\Lambda^*}{\Lambda} \ . \tag{1}$$

Since the pion is a Goldstone boson, its mass changes only slowly with density [10]. We have neglected this change.

Independently of these developments, Campbell, Ellis, and Olive [11] in their study of QCD phase transitions in an effective field model, arrived at the same conclusion about the scaling of hadron masses other than that of the pion, which they did not consider.

Given these theoretical motivations, it is of interest to see how this decrease in meson masses, Eq. (1), could have been concealed in the many analyses of standard processes in nuclear physics, which conventionally took the meson masses to be constant, independent of density. To this end, we shall, in this paper, reanalyze the scattering of protons by nuclei in the range of scattering energies 500–800 MeV. This is a formidable challenge, because the Dirac phenomenology and the relativistic IA2 have appeared to be extremely successful for just such experiments, initially in predicting not only differential cross sections but, in considerable detail, spin observables also. In the relativistic mean field theory, which we use as a guide, the scalar and vector mean fields are

$$S = \frac{g_S^2}{m_S^2}\rho_S \ , \quad V = \frac{g_V^2}{m_V^2}\rho_V \tag{2}$$

and the changes we propose amount to multiplying these by the density dependent factor $(m_N/m_N^*)^2$, which represents an $\sim 40\%$ effect at $\rho=\rho_0$.

We shall chiefly consider differential cross sections for proton-nucleus scattering, and show that with the assumption of the scaling, Eq. (1), these can be well fit provided allowance is made for the finite-range effects in the dynamical model [2,3] suggested to be responsible for the density dependence of the meson masses.

The density dependence of the meson masses results in a modification of the optical model potential. We can express this by making a transformation to an effective potential of increased strength but slightly decreased radius. This potential modification removes a long standing discrepancy in the nonrelativistic impulse approximation (NRIA) treatment (NRIA uses, however, relativistic kinematics) of proton-nucleus scattering at medium energies when densities derived from electron scattering are employed.

We make some qualitative observations about the expected changes in the imaginary part of the optical model potential and in the spin-orbit interaction, once the scaled meson masses are introduced.

Finally, showing the results of some recent relativistic calculations by Tjon and Wallace, we confirm that introduction of the scaled masses preserves their good IA2 fit to the cross section and spin observables in the example classic [12] to the relativistic treatment of 500 MeV proton scattering from ^{40}Ca.

II. THE NUCLEAR RADIUS DISCREPANCY

The chief discrepancy in the description of proton-nucleus scattering data by use of the NRIA is that radii slightly smaller than those obtained from electron scattering must be employed to obtain good fits. We show the comparison of the theory and experiment in Figs. 1–4.

We have performed NRIA calculations for comparison with the proton scattering data from ^{40}Ca and ^{58}Ni at 498 MeV and ^{208}Pb at 498 and 796 MeV. The folding and scattering calculations were performed with the programs ALLWORLD [13], and DWBA70 [14], respectively. The nucleon densities used in the folding calculations were determined as follows. The proton density, ρ_p, was obtained by unfolding the free proton charge form factor from the charge density deduced from electron scattering experiments. The neutron density, ρ_n, was computed from the equation

$$\rho_n=\frac{N}{Z}\rho_p+\left[\rho_n^D-\frac{N}{Z}\rho_p^D\right], \tag{3}$$

where $\rho_{n(p)}^D$ denotes the HFB neutron (proton) density of Decharge [15]. These densities were folded with the Love-Franey t matrix [16] to obtain the optical potential which was then used to calculate the proton-nucleus scattering. These "uncorrected" NRIA predictions for cross sections are shown in Figs. 1–4. The results for the differential cross section show a phase shift and underpredict the data at large θ for all targets at all energies.

A similar phase-shift discrepancy in K^+-^{12}C scattering was noted by Brown *et al.* [1], and removed by the introduction of density dependent vector meson masses following the suggestion of Abraham Gal [17]. We now sketch the resolution of this discrepancy.

In a local density approximation, which we shall need to improve upon below, the free K^+N t matrix is modified by the factor (in the linear approximation)

$$F=[1-\lambda\rho(r)/\rho_0]^{-1} \tag{4}$$

which, for small scattering angles, took into account the density dependence of the meson masses in the meson

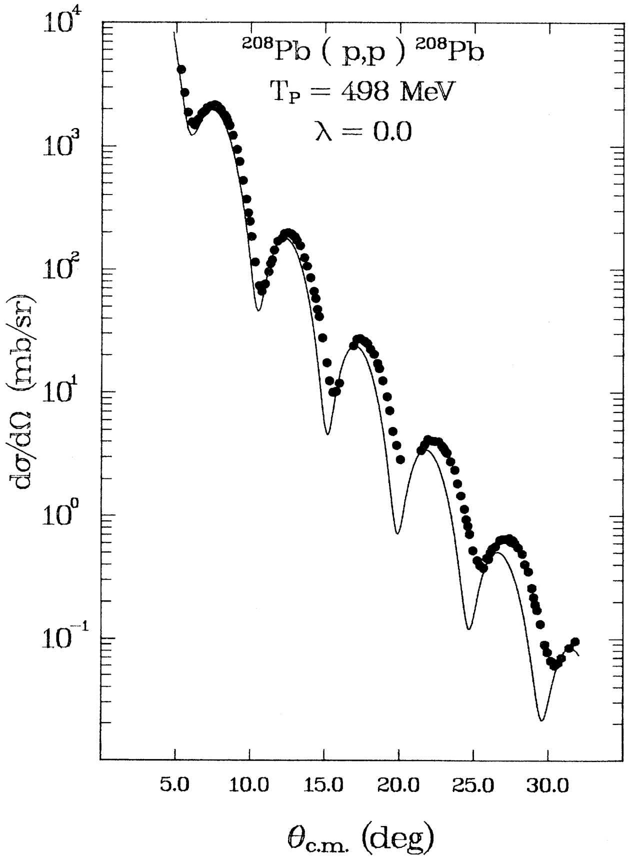

FIG. 1. Uncorrected nonrelativistic impulse approximation (NRIA) predictions for ^{208}Pb(p,p) elastic scattering cross section at T_p=498 MeV. The nucleon densities used were obtained as described in the text. The data are from Ref. [12].

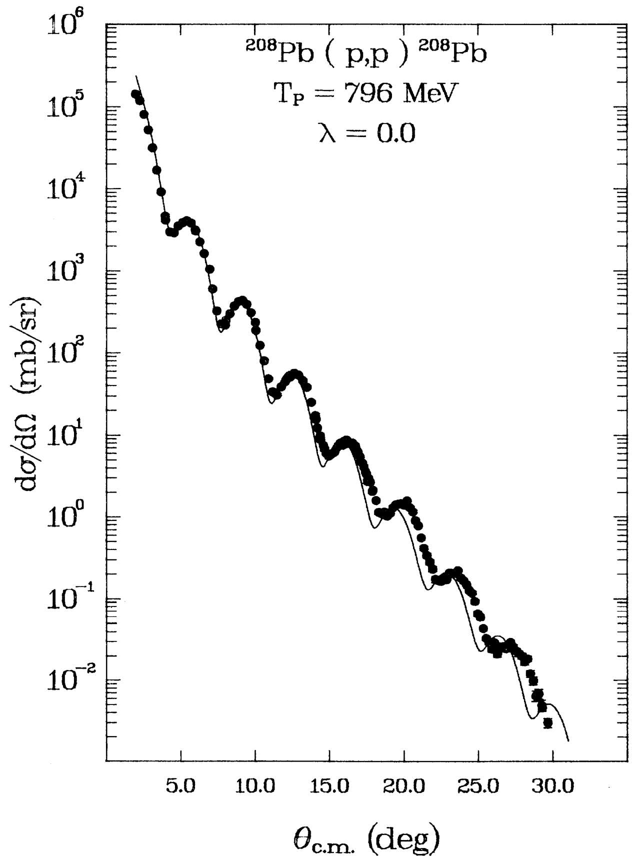

FIG. 2. Same as Fig. 1, but at 796 MeV. The data are from Refs. [34] and [35].

propagator. Here

$$\lambda = 2\left[1 - \frac{m_N^*(\rho_0)}{m_N}\right] . \tag{5}$$

Using an idea of Gibbs *et al.* [18], the factor F can be transformed away to the extent that the nucleon density can be represented by a two-parameter Fermi (2pF) function. The result is that the optical potential strength is increased by the factor $(1-\lambda)^{-1}$ (just the factor $[m_N/m_N^*(\rho(R=0))]^2$ referred to following Eq. (2)) and the half value radius R is replaced by an effective radius

$$R' = R - \lambda a \ , \tag{6}$$

where a is the diffuseness parameter. Basically, the product of two Fermi functions, one representing the optical model potential, and the other representing the $\rho(r)$ in Eq. (4) when expanded as

$$[1-\lambda\rho(r)/\rho_0]^{-1} \cong 1+\lambda\rho(r)/\rho_0,$$

has a thinner surface than a single Fermi function; hence, the foreshortening, Eq. (6), in R results from the effectively contracted surface thickness. It is surprising that the small change $\delta R = -\lambda a$ was substantially more decisive in bringing agreement between theory and experiment in the K^+-^{12}C scattering [1] than the much larger relative change in optical model potential. However, the charge distribution from ^{12}C is accurately known and extensive calculations [19,20] had been unable to reconcile the distribution of nucleons needed in the optical model with that obtained from the charge distribution. Consequently, in the case of K^+-^{12}C scattering, where conventional many-body effects are well under control because of the weakness of the known K^+N interaction, the density dependent meson masses played a crucial role in bringing theory into agreement with experiment. A more sophisticated calculation of K^+-^{12}C scattering has been done recently by Labarsouque [21] using the Brueckner reaction matrix and a K^+-nucleon potential built from a constituent quark model. This calculation showed little improvement over the impulse approximation. However, good agreement with the data was obtained by "swelling" the quark confinement radius and reducing the quark mass both with a $\lambda = 0.2$.

In the proton-nucleus scattering, interactions are much stronger than in the K^+-^{12}C scattering, but having established the role played by the density dependence of the meson masses there, one can look at proton scattering. There has been an even longer standing radius discrepancy problem there [22].

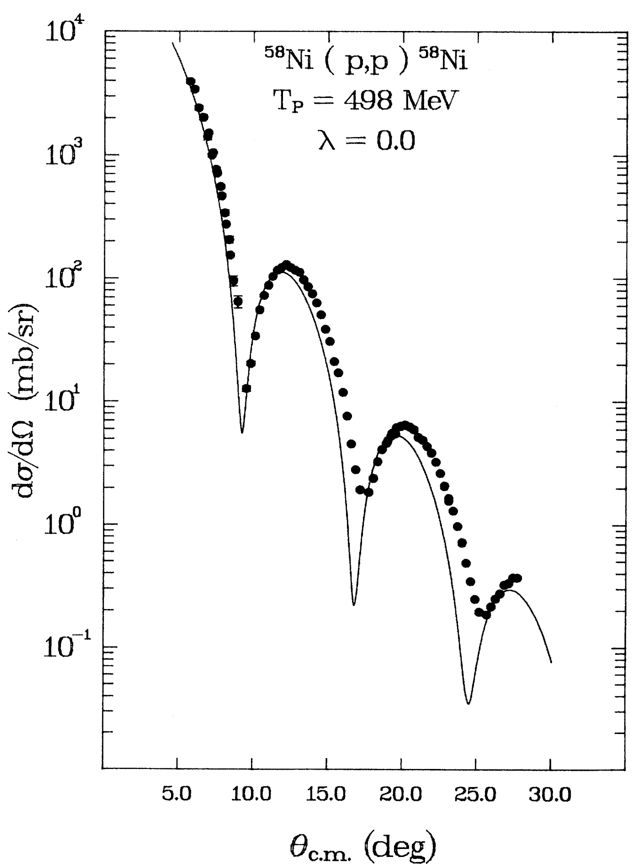

FIG. 3. Same as Fig. 1, but for ^{58}Ni at 498 MeV. The data are from Ref. [36].

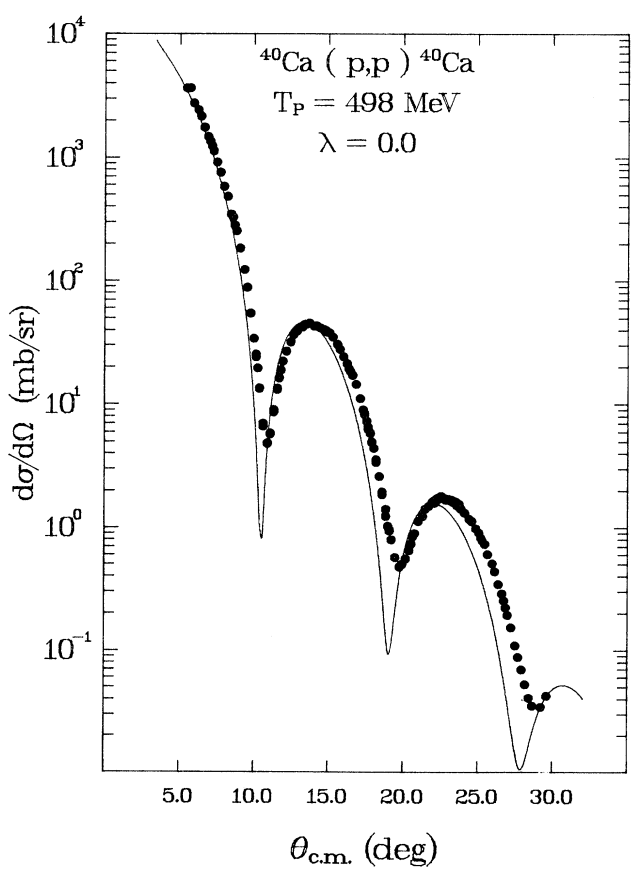

FIG. 4. Same as Fig. 1, but for ^{40}Ca at 498 MeV. The data are from Ref. [12].

Following the procedure pursued in the K^+-^{12}C analysis, we included the density dependence of the meson masses in the analysis of proton-nucleus scattering. Folding calculations were performed with a reduced effective density radius $R' = R - \lambda a$ for several values of λ. This was achieved by shrinking the densities $\rho_{p(n)}$ obtained above [Eq. (3)] by a percentage equal to $\lambda a/R$ (approximating the densities by a 2pF shape to obtain the equivalent a and R). The optical potentials obtained via folding were then multiplied by the enhancement factor $(1-\lambda)^{-1}$. This is equivalent to adding a ρ^2 term to the density as given below in Eq. (8). However, the factor used for the spin-orbit potential involved

$$\lambda_{\text{s.o.}} = \tfrac{3}{2}\lambda_{\text{central}} \tag{7}$$

for reasons which we give later after a discussion of the spin-orbit potential. The values of λ_{central} that give the best fits to the data were found to be 0.2 for ^{208}Pb at both the energies, and 0.3 for ^{40}Ca and ^{58}Ni. Attempts to find other values of λ which give good fits to the data were unsuccessful within the model constraints. Results and comparison with experiment are shown by the dashed lines in Figs. 5–8. It is clearly seen that with our λ's of 0.2–0.3, the radius discrepancy has largely been eliminated, at least with respect to the phase of the differential cross sections. (We return to a discussion of the amplitudes and of the related solid lines below.) The λ's that optimize the fits would give $m_N^*(\rho_0)/m_N = 0.9$ for ^{208}Pb and 0.85 for the other nuclei. This is substantially larger than values usually assumed for the nucleus effective mass at nuclear matter density, but in the same range as found in Ref. [1]. Similarly large values were found in the nuclear matter calculation of Ref. [23] where the largeness was caused by vacuum polarization effects. More conventionally, values $m_N^*(\rho_0)/m_N \le 0.8$ are arrived at, but, as we shall discuss later on, with corrections for finite range, our values decrease and some of the additional smallness in m_N^* may be mocking up effects from decreased meson masses. The values of λ we find here lie within the range needed to fit the K^+-^{12}C scattering [1].

The fact that our dotted lines lie above the experimental data for large θ could be anticipated from the detailed mechanism, Refs. [2] and [3], in which the $\rho(r)$-dependent corrections in

$$[1-\lambda\rho(r)/\rho_0]^{-1} \cong 1+\lambda\rho(r)/\rho_0$$

are derived from a three-body force involving a virtual $\Delta(33)$-isobar, nucleon-hole intermediate state. Applied to our present problem, this mechanism is shown in Fig.

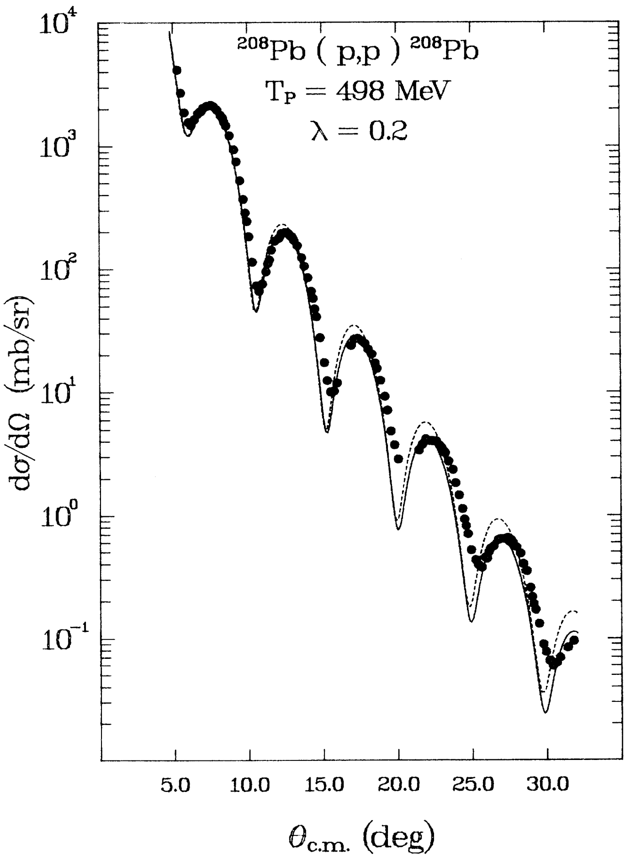

FIG. 5. Density dependent NRIA calculations with zero-range (dashed curve) and finite-range (solid curve) approximations for ^{208}Pb elastic scattering at $T_p = 498$ MeV. References for data are given in the captions for Figs. 1–4.

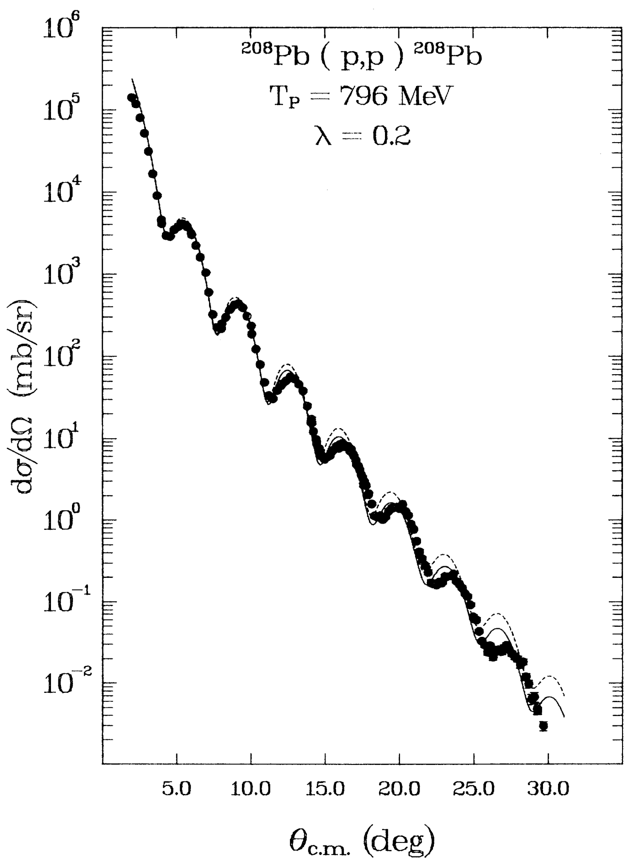

FIG. 6. Same as Fig. 5, but at $T_p = 796$ MeV.

9; the virtual isobar here arises from excitation of one of the target nucleons. It is readily checked that our expressions for the modification in optical model potential obtained earlier resulted from zero-range approximation in the meson lines shown in Fig. 9. Let us now go back and remove this approximation.

According to the argument of Ref. [2], the typical momentum of the virtual pion in these interactions is such that the virtual pion energy is $\approx 2m_\pi c^2$. (This estimate was very rough so we experimented somewhat to see whether changing this value would substantially alter the fits; it did not.) We replace the λ-dependent term in the IA,

$$\delta V_{\rm opt}(\mathbf{r})=\frac{\lambda}{\rho_0}\int t(\mathbf{r}-\mathbf{r}_i)\rho^2(\mathbf{r}_i)d^3\mathbf{r}_i \tag{8}$$

by

$$\delta V_{\rm opt}=\frac{\lambda m_\pi^2}{\pi\rho_0}\int\int d^3\mathbf{r}_i d^3\mathbf{r}_j t(\mathbf{r}-\mathbf{r}_i)\times\frac{e^{-2m_\pi|\mathbf{r}_i-\mathbf{r}_j|}}{|\mathbf{r}_i-\mathbf{r}_j|}\rho(\mathbf{r}_i)\rho(\mathbf{r}_j) \tag{9}$$

where $\mathbf{r}$ denotes the coordinates of the incident proton, $\mathbf{r}_i$ and $\mathbf{r}_j$ represent the target nucleons involved in scattering, m_π is the pion mass, ρ_0 is the central nuclear density and t denotes the Love-Franey t matrix [16]. This extra term, $\delta V_{\rm opt}$, is added to the potential $V_{\rm opt}$ obtained in the "uncorrected" NRIA and the resulting optical potential is then used to calculate the scattering observables. The calculations are done using the same values of λ as in the "zero-range" case and once again $\lambda_{\rm s.o.}=\frac{3}{2}\lambda_{\rm central}$ is assumed. The results of such "finite-range" calculations are shown in Figs. 5–8 (solid curves) for the nuclei of interest. These show a significant improvement over the previous "zero-range" calculations (dashed curves, Figs. 5–8) in both the phase as well as the magnitude of the cross section.

The greatest success of the effect of medium modification of meson masses appears to be in the 500 MeV energy region where both the phase and the magnitude of the cross sections are reasonably well reproduced. At 796 meV the calculations slightly over predict the cross section maxima at large angles.

The improvement in fits to the data using the finite range estimated in Ref. [2] is important because whereas general fundamental arguments such as those given in Ref. [11] show that meson masses should decrease with density in the movement towards chiral restoration, they give no indication as to the precise mechanisms by which this is accomplished in the variables appropriate to the

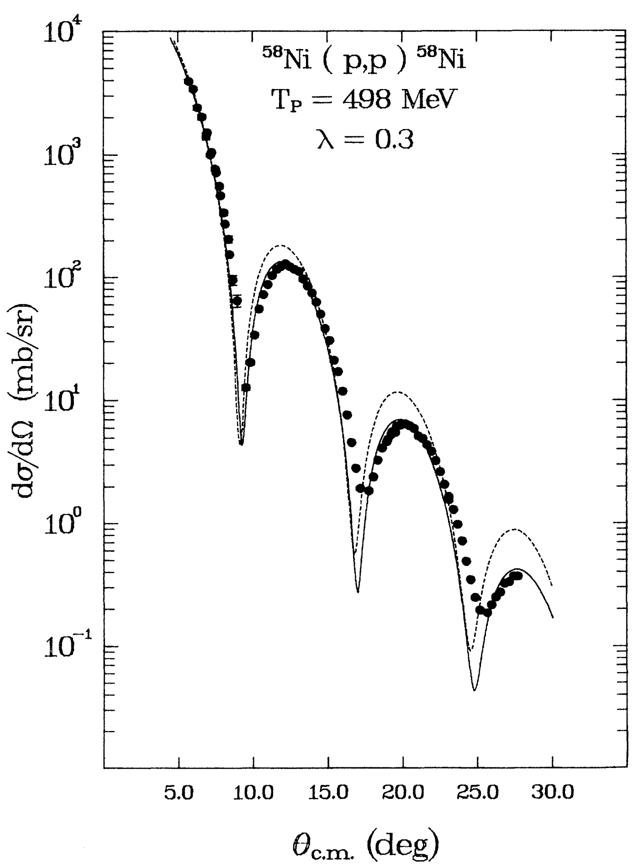

FIG. 7. Same as Fig. 5, but for ^{58}Ni at $T_p=498$ MeV.

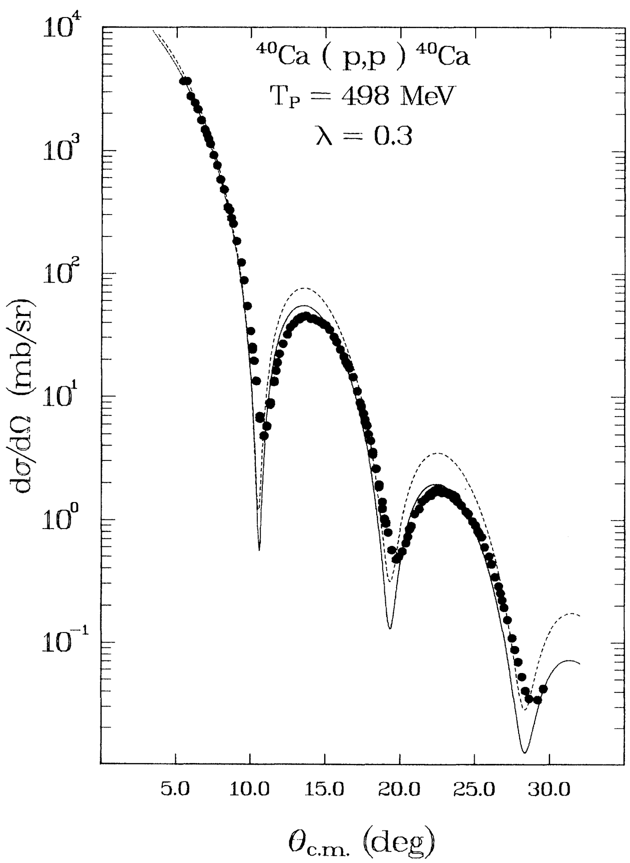

FIG. 8. Same as Fig. 5, but for ^{40}Ca at $T_p=498$ MeV.

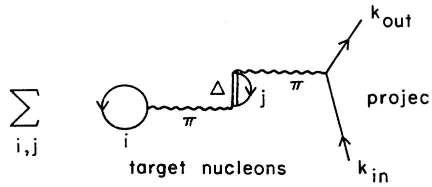

FIG. 9. A typical ρ^2 term arising from medium dependence in the interaction. These will generally be accompanied by at least one additional virtual pion exchange, so our treatment here is somewhat schematic.

broken symmetry (meson, nucleon) sector. We see that the arguments of Ref. [2] do give about the correct range for the needed finite-range corrections. However, this range of $\sim\hbar/2m_\pi c$ is appreciable, so we also understand that our decreased meson masses cannot be directly applied to few-body systems, but, rather, three-body forces should be explicitly introduced, as is often done. In a sense, the arguments of Ref. [2] demystify the relation, Eq. (1), by explaining the decrease in meson masses in terms of three-body forces, such as are often employed.

III. THE SPIN-ORBIT INTERACTION

Although the behavior of the spin-orbit interaction is not central to our problem, we should explain Eq. (7), i.e., why we scaled it differently than the central potential. Also, the spin-orbit interaction is generally of interest, because until the advent of relativistic theories, the calculated spin-orbit splittings in nuclei were much smaller than the empirical ones, and one of the great apparent successes of the relativistic theories, such as the Walecka theory, was in removing this discrepancy.

The spin-orbit interaction in relativistic mean field theory goes as [24]

$$U_{\text{s.o.}} = -\frac{1}{2m_N m_N^*}\frac{\sigma\cdot 1}{r}\frac{d}{dr}(S-V) . \tag{10}$$

As is well known, this is large because S and V are of opposite sign. Furthermore, the enhancement from a small effective mass, $m_N^* \le 0.6 m_N$ in relativistic mean field theory produces a large enough spin-orbit splitting of valence levels to fit the empirical values. We have a much larger effective mass $m_N^* \sim 0.85 m_N$. However, at least in mean field approximation, since our mean fields are increased by the factor $(m_N/m_N^*)^2$, we find

$$U_{\text{s.o.}}(m_N^*, m_m^*) = \left[\frac{m_N}{m_N^*}\right]^3 U_{\text{s.o.}}(m_N, m_m) . \tag{11}$$

Thus, at nuclear matter density ρ_0, with our $(m_N^*/m_N)=0.85$, we get a factor of 1.63 increase to be compared with the factor of 1.67 from Walecka mean field theory with $(m_N^*/m_N)=0.6$. To get a large enough density of states at the Fermi surface

$$\rho(E_F) = 2k_F m_N^*/\pi^2 , \tag{12}$$

it is, in general, helpful to have our larger m_N^*, since the empirical density of states in medium and heavy nuclei requires $m_N^*/m_N \ge 1$. A significant amount of this large m_N^* comes, however, from the coupling of the quasiparticles to vibrations, so it is difficult to argue quantitatively. The m_N^* needed to fit the energy dependence of the proton-nucleus scattering in the few hundred MeV region is somewhat smaller [25] than our value of $m_N^*/m_N=0.85$. In any case, the fact that the cube of (m/m^*) comes into Eq. (11) is generally helpful in obtaining a large spin-orbit interaction which seems useful not only in getting large enough spin-orbit splittings in nuclei, but also in reproducing the spin observables in high energy proton nucleus scattering.

IV. THE IMAGINARY PART OF THE OPTICAL MODEL POTENTIAL

New elements enter into the imaginary part of the optical model potential which are not properly taken into account by our increase of the overall optical model potential by the factor of $(1-\lambda)^{-1}$, which the scaling of the meson masses effectively does. Whereas we have not solved this problem, we wish to raise the issue here.

In the nonrelativistic impulse approximation, the imaginary potential comes from the imaginary part of the two-body t matrix

$$U_I = (\text{Im}t)\rho , \tag{13}$$

where $t(q=0)$ can be used since the range of q is restricted by ρ to be $\sim 1/R$, with R being the nuclear radius. From the optical theorem,

$$\sigma_{NN} = \frac{4\pi}{k}\text{Im}t(q=0) , \tag{14}$$

where σ_{NN} is the two-body total cross section. It is obtained, in Born approximation (which should be adequate for our discussion), by integrating over angles the differential cross sections

$$\frac{d\sigma}{d\Omega} = \frac{m_N^2}{4\pi\hbar^2}|V_{k'-k}|^2 . \tag{15}$$

Note that if m_N goes to m_N^* in the medium, a correction seldom put in, the $d\sigma/d\Omega$ would be substantially cut down.

In Eq. (15)

$$V_{k'-k} = \frac{g_i^2}{m_i^2+q^2}, \quad q=k'-k , \tag{16}$$

where g_i and m_i are the relevant meson coupling constant and mass (e.g., for scalar and vector mesons). With the assumption, Eq. (1), that meson masses scale with density like the nucleon mass, one finds that the ratio R of in-medium to free two-body differential cross sections is

$$R(q) = \left[\frac{m_N^*}{m_N}\right]^2 \left[\frac{m_i^2+q^2}{\left[\frac{m_N^*}{m_N}\right]^2 m_i^2+q^2}\right]^2 . \tag{17}$$

One of the factors m_N^*/m_N comes from the *in-medium* density of final states and should be present, whereas the

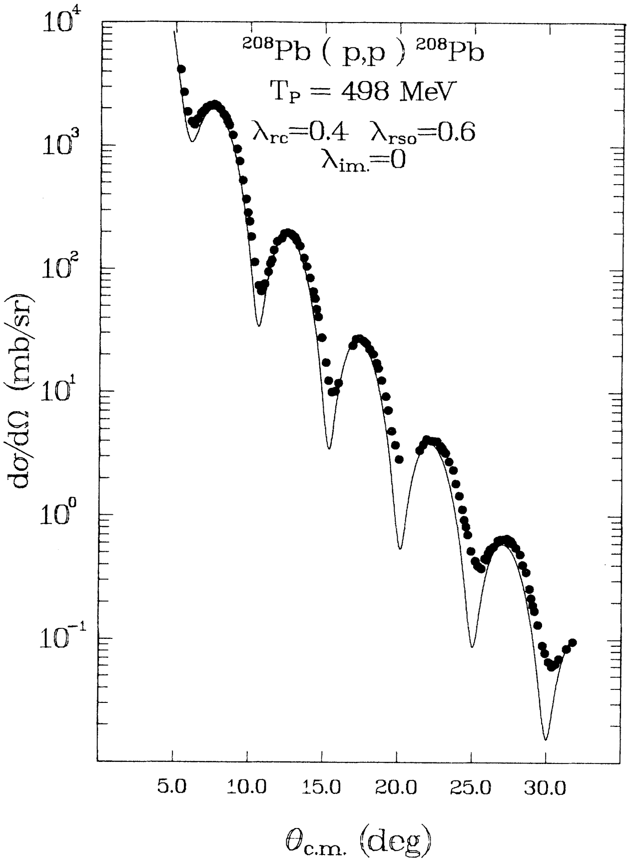

FIG. 10. Density dependent NRIA calculation with finite-range approximation and $\lambda_{imag}=0$ (for both central and spin-orbit potentials) for ^{208}Pb elastic scattering at $T_p=498$ MeV. For real potentials, $\lambda_{central}=0.4$ and $\lambda_{s.o.}=0.6$ were used.

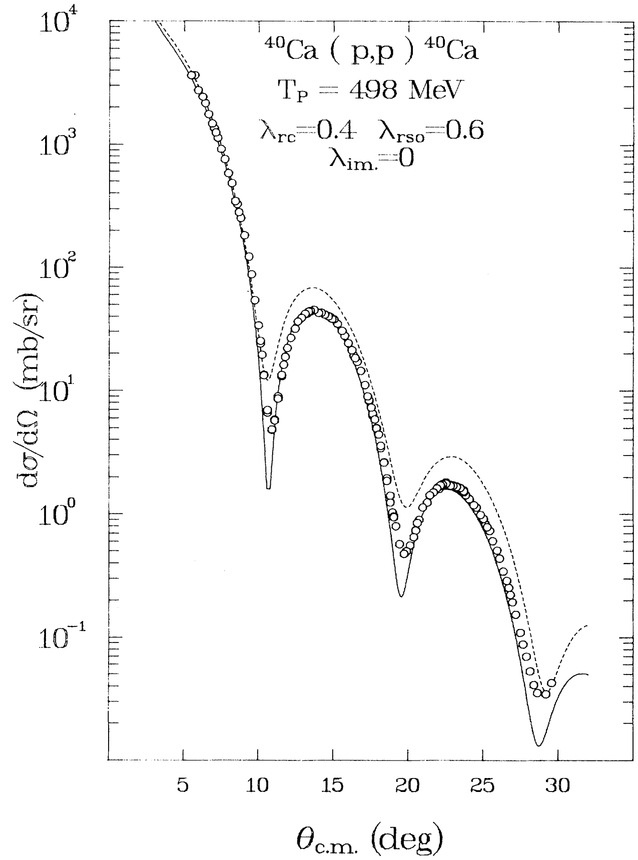

FIG. 11. Same as Fig. 10, but for ^{40}Ca at $T_p=498$ MeV. Calculations with zero-range (dashed curve) and finite-range (solid curve) approximations are shown.

other factor originates from the flux, and, from Galilean invariance, this factor will be restored to unity once backflow is included. As is well known, the current of a particle of momentum p is $j=p/m_N$, not $j=p/m_N^*$.

There is considerable cancellation between the m_N^*/m_N in the numerator of Eq. (17) and the m_i^{*2} in the denominator. Generally, the m_N^*/m_N is not taken into account, although even in the conventional scenarios it should be, because the *in-medium* density of states is smaller than that in free space. On the other hand, meson effective masses are also not included in conventional calculations, as we suggest they should be.

In calculations shown in Figs. 10 and 11, we have explored the consequences of leaving the imaginary part of the optical model potential unchanged; i.e., not increasing it by the factor of $(1-\lambda\rho/\rho_0)^{-1}$. Quite credible fits are obtained for $T_p=498$ MeV for both ^{208}Pb and ^{40}Ca, and we are now able to increase λ to 0.4; i.e., lower $m_N^*(\rho_0)/m_N$ to 0.8. The theoretical minima in the finite range calculation are too deep, indicating that possibly U_I should be increased somewhat.

We do not claim to have resolved the issue of how U_I should scale, but only wish to indicate that effects, other than those conventionally included, should be considered. Probably U_I should increase by a factor of between unity and $(1-\lambda\rho/\rho_0)^{-1}$.

V. DISCUSSION

In this paper we have used the nonrelativistic impulse approximation, but with relativistic kinematics, to study the influence of density dependent meson masses on the differential cross section. Since here we are concerned with the simple problem of diffraction by a complex potential, the NRIA should be sufficient to study this problem.

The question immediately arises, however, as to how the spin observables, which are reproduced so well by Dirac phenomenology, are influenced by the medium dependent meson masses. We were unable to answer this question, because NRIA does poorly in reproducing spin variables. However, Tjon and Wallace [26] have used our prescription of decreasing the meson masses in their relativistic IA2 formalism [27]. We show their results for $\lambda=0.3$ in Figs. 12 and 13. Note that for the differential cross section shown in Fig. 12 that there is the same tendency for the solid line, which treats the scaling meson masses in zero-range approximation, to over predict the data at the larger angles as we found in the nonrelativistic zero-range approximation. Tjon and Wallace [26] have

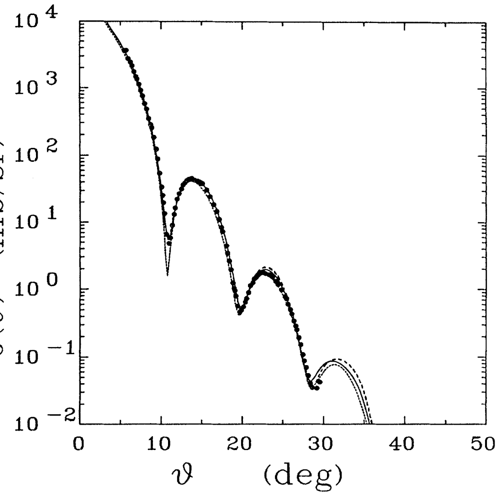

FIG. 12. Preliminary results of Tjon and Wallace [26] for the differential cross section of 500 MeV protons scattered elastically from ^{40}Ca. The dotted curve gives the IA2 results. For the solid curve, a linear scaling with density was assumed, with $m_\sigma^*(\rho_0)/m_\sigma = m_\omega^*(\rho_0)/m_\omega = m_\rho^*(\rho_0)/m_\rho = 0.85$. For the dashed line, m_σ and m_ω were scaled in this way, but m_ρ was held constant at its $\rho=0$ value.

not yet included the finite-range correction, but for the relatively small $\lambda=0.3$ the effect may not be large. In Fig. 13, one can see that the quality of fit to the polarization observables does not worsen in going from the IA2 results to the ones with density dependent masses. No attempt was made to readjust parameters in this calculation; the medium dependent meson masses were simply inserted into the IA2 code. The goodness of fit with our assumption [Eq. (1)] is probably not an accident. This

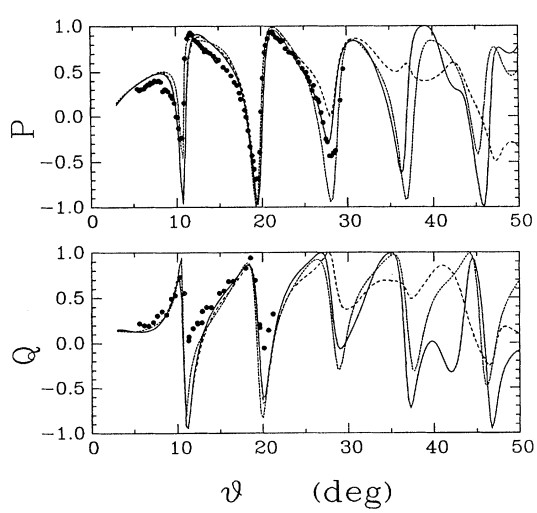

FIG. 13. Results of Tjon and Wallace [26] for the spin observables, for 500 MeV protons scattered elastically from ^{40}Ca. The various lines have the same meaning as in the caption to Fig. 12.

can be seen from the dashed curve in Fig. 13, where the σ and ω masses are taken to scale with density as in Eq. (1), but m_ρ is taken to be constant. Although ρ-meson exchange is generally not thought to be important in Dirac phenomenology, it is included in IA2, and it can be seen from Fig. 13 that the fit to the polarization data is significantly worsened if m_ρ does not scale with m_ω and m_σ. In these calculations the pion mass (m_π) was not scaled, following the conclusion of Nambu [10] that the pion mass varies only little with density, increasing only 5 MeV as ρ increases from 0 to ρ_0. Whereas IA2 does not explicitly include an effective nucleon mass m_N^*, it does keep positive and negative energy states, in a plane wave decomposition. In Ref. [28] it was shown that in perturbation theory this was equivalent to use of a nucleon effective mass in Walecka mean field theory and in Ref. [29] this was shown to be quantitatively accurate (beyond perturbation theory) in the Bonn boson exchange model in the nuclear many-body problem. The IA2 scalar potential at 500 meV incident proton energy is [30], however, -210 MeV, which would correspond to an effective mass of 0.79, so the nucleon effective mass m_N^* is a bit smaller than the $m_N^*/m_N=0.85$ used for most of our figures and, in particular for the IA2 results, Figs. 12 and 13. Our results in Fig. 11 show that we can perfectly well tolerate $m_N^*/m_N=0.80$ for acceptable (lack of) change in the imaginary part of the optical model potential. We were only able to reduce m_N^*/m_N down to 0.80 after corrections for finite range were made in the NRIA.

In any case, the scaling [Eq. (1)] is only approximate. This is clear from the derivation of the scaling in the QCD sum rule approach of Ref. [9]. In the calculations to date in this formalism, the continuum is approximated by the perturbative one, and calculations in progress show that in the case of the nucleon, this is not a good approximation (although it appears to be in the case of the vector meson). However, the work of Ref. [11] shows that there is only one way to introduce a scale in the broken symmetry mode through breaking the scale invariance in the underlying QCD through the trace anomaly, so that there is a good fundamental foundation for Eq. (1). On the phenomenological side, the preliminary results [26] for the spin observables should be sufficiently encouraging to stimulate further work.

We are unaware of systematic studies in the relativistic IA1 or IA2 formalisms employing empirical nuclear density distributions obtained from electron scattering. To the extent that many of these calculations employ nuclear density distributions calculated from Walecka mean field theory, the nuclear radius discrepancy would not have been noticed. The unphysically large compression modulus, $K \simeq 500$ MeV, commonly used in these calculations would give a thin surface thickness just as do our density dependent meson masses as discussed following Eq. (6). Of course, calculations in which nuclear density parameters were fit in order to reproduce data would also not have shown this discrepancy. The nuclear radius discrepancy could probably be fixed up in any given nucleus by a variety of higher-order effects, but we believe it to be important that following the procedure of Ref. [1]

where, in K^+-^{12}C scattering, higher order effects are well under control, we achieve a resolution of this discrepancy.

VI. CONCLUSIONS

Simple estimates, based on nonrelativistic impulse approximations (but with relativistic kinematics) are presented in this paper. They suggest that two interesting features might emerge from the density dependence of meson masses: first, the effective radius of the optical potential can be altered by a small, but significant amount; and second, the scalar and vector potentials can be increased.

With respect to the first feature, we believe our use of NRIA to be adequate to discuss differential cross sections. It is clearly inadequate for spin observables. For these an approach along the lines of the Tjon-Wallace IA2 should be employed. It is necessary to determine a new form of optical potential, beginning from the *NN* *t*-matrix, consistently generalized to include the density dependence of the meson masses. First results of Tjon and Wallace [26] in this direction indicate that introduction of scaling masses does not worsen the good agreement of IA2 for the scattering of 500 MeV protons by ^{40}Ca. Clearly a more extensive investigation is necessary to properly assess the quantitative validity of our scenario. The promising first results of Tjon and Wallace should stimulate this.

With respect to the second feature, increased scalar and vector potentials, we note that those commonly employed in Dirac Phenomenology are $\gtrsim 50\%$ larger in magnitude than the IA2 scalar and vector potentials. In a naive approach, in which these mean fields arise as g^2/m^2, where g is the scalar or vector coupling constant and m is the relevant meson mass, we would expect an *in medium* enhancement of the IA2 scalar and vector potentials by the factor $(m/m^*)^2$. In our case this enhancement is density dependent, entering in a more complicated way than by an overall factor. Nevertheless, indications are that such enhanced potentials fit the data well.

Our discussion in this paper was almost completely phenomenological, but we outlined in the introduction the conceptual arguments which led to the introduction of density dependent effective masses.

After completion of this work we received the preprint [31] from Hosaka and Toki, "*G*-matrix elements with effective masses for mesons and nucleons." Their conclusion is that, "A uniform decrease in various masses yields *G*-matrix elements which are rather consistent with empirical matrix elements obtained by Brown, Richter, Julies and Wildenthal" [32].

ACKNOWLEDGMENTS

We would particularly like to thank John Tjon and Steve Wallace for carrying out the calculations shown in Figs. 12 and 13, and for communicating them to us. We would like to thank B. C. Clark, M. A. Franey, W. G. Love, M. Rho, E. Rost, J. R. Shepard, and S. J. Wallace for several helpful discussions. We are also grateful to Rost, Shepard, and Wallace for providing us with their relativistic nucleon-nucleus scattering programs. This work was supported in part by U.S. Department of Energy Grant Nos. DE-FG02-88ER40388 and DE-FG02-88ER40405 and the Minnesota Supercomputer Institute.

APPENDIX

Here we examine the effect of density dependent meson masses in the electromagnetic form factor.

In the text of the article, the effect of density dependent meson masses on the electromagnetic form factor has been neglected. If nucleon density distributions are to be taken from electron scattering off nuclei, corrections should be made. We shall show here that this correction is substantially less than that given by the factors of $(m/m^*)^2$ discussed in the text.

It is known that strength is missing in the longitudinal form factor for electron scattering from nuclei. Let us first consider that in this scattering the virtual γ-ray always couples through vector mesons. Thus, the isoscalar form factor (see Fig. 14) will be

$$F_{\mathrm{VDM}}^{I=0}=\frac{1}{1+q^2/m_\omega^2}\ , \tag{A1}$$

where VDM stands for vector dominance model. If the *in medium* modification is described by letting $m_\omega \to m_\omega^*$, then the difference between the modified and unmodified form factor is

$$\delta F_{\mathrm{VDM}}=F_{\mathrm{VDM}}^{I=0}(m_\omega)-F_{\mathrm{VDM}}^{I=0}(m_\omega^*)=\frac{q^2}{m_\omega^{*2}}-\frac{q^2}{m_\omega^2}\ . \tag{A2}$$

The expansion is justified, because only $q \sim R^{-1}$, where R is the nuclear radius, enter.

Keeping the q dependence in meson propagators changes the factor of $(m/m^*)^2$ enhancement in our mean fields [see Eq. (2) and the following discussion] into

$$\begin{aligned} F&=\left[\frac{m}{m^*}\right]^2\left[\frac{1+q^2/m^2}{1+q^2/m^{*2}}\right]\\ &\simeq\left[\frac{m}{m^*}\right]^2\left[1+\frac{q^2}{m^2}-\frac{q^2}{m^{*2}}\right], \end{aligned} \tag{A3}$$

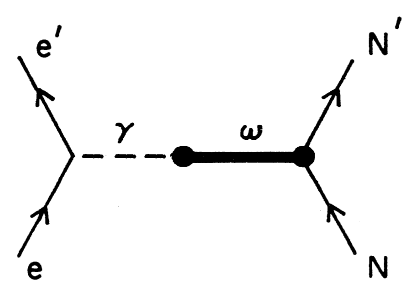

FIG. 14. In electron scattering, the virtual γ-ray couples through vector mesons in the vector dominance model. Here the isoscalar coupling, through the ω meson is shown. The large solid dots indicate form factors.

where m and m^* are the free and effective mass of the exchanged meson. To the extent that the meson mass is close to m_ω, the q-dependent factors in F_{VDM} and F cancel. In any case, the q-dependent correction is smaller than the leading one by a factor of $[1-(m^*/m)^2](m_\omega R)^{-2}$.

Brown and Rho [33] point out that for small spacelike momenta the vector meson in Fig. 14 is substantially off shell. They estimate that, because of this, the γ-ray couples only $\sim\frac{1}{2}$ the time through vector mesons; the other half of the time it couples, as a γ ray, directly to the quarks in the internal structure (e.g., little bag) of the nucleon. With this scenario, the q-dependent correction in the electromagnetic coupling $A(2)$ is only $\sim\frac{1}{2}$ that for the nucleus, e. g., $A(3)$. In this case, the q^2 correction can be compensated for by increasing λ a few percent.

[1] G. E. Brown, C. B. Dover, P. B. Siegel, and W. Weise, Phys. Rev. Lett. **60**, 2723 (1988).
[2] T. L. Ainsworth, G. E. Brown, M. Prakash, and W. Weise, Phys. Lett. B **200**, 413 (1988).
[3] G. E. Brown, Prog. Theor. Phys. Suppl. **91**, 85 (1987); Nucl. Phys. **A507**, 251c, (1990).
[4] G. E. Brown and M. Rho, Phys. Lett. **222**, 324 (1989).
[5] G. E. Brown and M. Rho, Phys. Lett. **237**, 3 (1990).
[6] V. Bernard, U.-G. Meissner, and I. Zahed, Phys. Rev. Lett. **59**, 966 (1987).
[7] V. Bernard and U.-G. Meissner, Nucl. Phys. **A489**, 647 (1988).
[8] C. Adami and G. E. Brown, submitted to Z. Phys.
[9] G. E. Brown, in Proceedings of the Akito Arima Symposium, 1990 [Nucl. Phys. A (to be published)].
[10] Y. Nambu, in *FestiVal-Festschrift for Val Telegdi,* edited by K. Winter (Elsevier, New York, 1988).
[11] B. A. Campbell, John Ellis, and K. A. Olive, Phys. Lett. B **235**, 325 (1990); Nucl. Phys. **B345**, 57 (1990).
[12] G. W. Hoffman *et al.,* Phys. Rev. Lett. **47**, 1436 (1981); K. K. Seth *et al.,* Phys. Lett. **158B**, 23 (1985); J. R. Shepard, J. A. McNeil, and S. J. Wallace, Phys. Rev. Lett. **50**, 1443 (1983).
[13] J. Carr, F. Petrovich, and J. Kelly, computer program ALLWORLD (unpublished).
[14] R. Schaeffer and J. Raynal, computer program DWBA70 (modified); J. Raynal, Nucl. Phys. **A97**, 572 (1967).
[15] J. Dechargé, CEA-N-260, Centre d'Etudes de Bruyeresle-Chatel (1982); J. Dechargé and D. Gogny, Phys. Rev. C **21**, 1568 (1980).
[16] M. A. Franey and W. G. Love, Phys. Rev. C **31**, 488 (1985).
[17] Abraham Gal, private communication.
[18] W. R. Gibbs, B. F. Gibson, and G. J. Stephenson, Phys. Rev. Lett. **39**, 1316 (1977).
[19] D. Marlow *et al.,* Phys. Rev. C **25**, 2619 (1982).
[20] P. B. Siegel, W. B. Kaufman, and W. R. Gibbs, Phys. Rev. C **30**, 1256 (1984).
[21] J. Labarsouque, Universite de Bordeaux I, report, 1989; W. Weise, Il. Nuovo Cimento **102A**, N.1, 265 (1989).
[22] N. M. Hintz *et al.,* Univ. of Minnesota Annual Report, 1983–84 (unpublished), p. 17; N. M. Hintz *et al.,* Univ. of Minnesota, Summary Progress Report, 1984–87, (unpublished), p. 51.
[23] G. E. Brown, H. Müther, and M. Prakash, Nucl. Phys. **A506**, 565 (1990).
[24] B. D. Serot and J. D. Walecka, *Advances in Nuclear Physics,* edited by J. W. Negele and E. Vogt (Plenum, New York, 1985), Vol. 16.
[25] N. Hintz, in *Proceedings of the University of Pittsburgh Conference on Nuclear Structure,* edited by S. Meshkov, 1957 (Univ. of Pittsburgh, Pittsburgh, 1957).
[26] J. A. Tjon and S. J. Wallace, private communication.
[27] J. A. Tjon and S. J. Wallace, Phys. Rev. C **36**, 1085 (1987).
[28] G. E. Brown, W. Weise, G. Baym, and J. Speth, Comments Nucl. Part. Phys. **17**, 39 (1987).
[29] R. Machleidt, in *Advances in Nuclear Physics,* edited by J. W. Negele and W. Vogt (Plenum, New York, 1989), Vol. 19, p. 189.
[30] N. Ottenstein, S. J. Wallace, and J. A. Tjon, Phys. Rev. C **38**, 2272 (1988).
[31] A. Hosaka and H. Toki, University of Pennsylvania Report 0449T, 1990.
[32] B. A. Brown, W. A. Richter, R. E. Julies, and B. H. Wildenthal, Ann. Phys. **182**, 191 (1988).
[33] G. E. Brown and Mannque Rho, Phys. Lett. **222**, 324 (1989).
[34] M. M. Gazzaly *et al.,* Phys. Rev. C **25**, 408 (1982).
[35] G. W. Hoffman *et al.,* Phys. Rev. C **21**, 1488 (1980).
[36] N. M. Hintz *et al.,* Phys. Rev. C **30**, 1976 (1984).